

RESEARCH ARTICLE

Maternal pomegranate juice intake and brain structure and function in infants with intrauterine growth restriction: A randomized controlled pilot study

Lillian G. Matthews^{1*}, Christopher D. Smyser^{2,3,4}, Sara Cherkerzian⁵, Dimitrios Alexopoulos³, Jeanette Kenley², Methodius G. Tuuli⁶, D. Michael Nelson⁶, Terrie E. Inder¹

1 Department of Pediatric Newborn Medicine, Brigham and Women's Hospital, Harvard Medical School, Boston, Massachusetts, United States of America, **2** Department of Pediatrics, Washington University, Saint Louis, Missouri, United States of America, **3** Department of Neurology, Washington University, Saint Louis, Missouri, United States of America, **4** Mallinckrodt Institute of Radiology, Washington University, Saint Louis, Missouri, United States of America, **5** Department of Medicine, Brigham and Women's Hospital, Harvard Medical School, Boston, Massachusetts, United States of America, **6** Department of Obstetrics and Gynecology, Washington University, Saint Louis, Missouri, United States of America

* lmattews4@bwh.harvard.edu



OPEN ACCESS

Citation: Matthews LG, Smyser CD, Cherkerzian S, Alexopoulos D, Kenley J, Tuuli MG, et al. (2019) Maternal pomegranate juice intake and brain structure and function in infants with intrauterine growth restriction: A randomized controlled pilot study. *PLoS ONE* 14(8): e0219596. <https://doi.org/10.1371/journal.pone.0219596>

Editor: Umberto Simeoni, Centre Hospitalier Universitaire Vaudois, FRANCE

Received: December 11, 2018

Accepted: March 24, 2019

Published: August 21, 2019

Copyright: © 2019 Matthews et al. This is an open access article distributed under the terms of the [Creative Commons Attribution License](https://creativecommons.org/licenses/by/4.0/), which permits unrestricted use, distribution, and reproduction in any medium, provided the original author and source are credited.

Data Availability Statement: Data cannot be shared publicly because we had not previously sought IRB approval for public sharing of participant data as part of our informed consent. However we will gladly share with any investigator the de-identified minimal raw data set needed to replicate the study upon request. Requests for sharing and access of data should be directed to: Sydney Kaplan, 660 South Euclid Avenue, Campus Box 8111, St. Louis, MO 63110-1093, Email: sydney.kaplan@wustl.edu.

Abstract

Polyphenol-rich pomegranate juice has been shown to have benefit as a neuroprotectant in animal models of neonatal hypoxic-ischemia. No published studies have investigated maternal polyphenol administration as a potential neuroprotectant in at-risk newborns, such as those with intrauterine growth restriction (IUGR). This was a randomized, placebo-controlled, double-blind pilot study to investigate the impact of maternal pomegranate juice intake in pregnancies with IUGR, on newborn brain structure and function at term-equivalent age (TEA). Mothers with IUGR at 24–34 weeks' gestation were recruited from Barnes-Jewish Hospital obstetrical clinic. Consented mothers were randomized to treatment (8 oz. pomegranate juice) or placebo (8 oz. polyphenol-free juice) and continued to take juice daily from enrollment until delivery (mean 20.1 and 27.1 days, respectively). Infants underwent brain MRI at TEA (36–41 weeks' gestation). Brain measures were compared between groups including: brain injury score, brain metrics, brain volumes, diffusion tensor imaging and resting state functional connectivity. Statistical analyses were undertaken as modified intention-to-treat (including randomized participants who received their allocated intervention and whose infants received brain MRI) and per-protocol (including participants who strictly adhered to the protocol, based on metabolite status). Seventy-seven mothers were randomized to treatment (n = 40) or placebo (n = 37). Of these, 28 and 27 infants, respectively, underwent term-equivalent MRI. There were no group differences in brain injury, metrics or volumes. However, treatment subjects displayed reduced diffusivity within the anterior and posterior limbs of the internal capsule compared with placebo. Resting state functional connectivity demonstrated increased correlation and covariance within several networks in treatment subjects, with alterations most apparent in the visual network in per-protocol analyses. Direct effects on health were not found. In conclusion, maternal

Funding: This work was supported by National Institute of Health Grants R01 HD29190 (D. M. Nelson), K02 NS089852 (C.D. Smyser), U54 HD087011 and P30 HD062171 (T.E. Inder), The Foundation for Barnes-Jewish Hospital (D. M. Nelson) and an unrestricted gift to Washington University School of Medicine from POM Wonderful, Los Angeles, CA. The funders had no role in study design, data collection and analysis, decision to publish, or preparation of the manuscript.

Competing interests: The authors have declared that no competing interests exist.

pomegranate juice intake in pregnancies with known IUGR was associated with altered white matter organization and functional connectivity in the infant brain, suggesting differences in brain structure and function following *in utero* pomegranate juice exposure, warranting continued investigation.

Clinical trial registration. [NCT00788866](https://www.clinicaltrials.gov/ct2/show/study/NCT00788866), registered November 11, 2008, initial participant enrollment August 21, 2012.

1. Introduction

Hypoxic-ischemic injury is the most common contributor to brain injury in the term-born infant. Occurring in 2 per 1000 live births, it results in substantial morbidity and mortality, contributing to almost a quarter of newborn deaths worldwide [1–3]. Despite advances in neonatal intensive care, including recent widespread implementation of therapeutic hypothermia [2, 4, 5], as many as 35% of survivors experience significant long-term neurodevelopmental deficits [3, 5, 6].

Oxidative stress represents a key pathophysiological mechanism in hypoxic-ischemic neuronal injury involving free radical production and a destructive inflammatory cascade [7], with devastating consequences on the developing brain [8]. Critically, brain injury following hypoxic-ischemia is a dynamic process, evolving over hours to weeks [9]. By the time an infant with injury presents secondary degeneration has often already commenced [10, 11], limiting the potential benefit of neuroprotective strategies started *ex utero*. Shifting treatment focus to the fetus *in utero* thus represents a unique window for therapeutic intervention in hypoxic-ischemia.

Polyphenols are a promising class of neuroprotectants shown to exert their effects directly on the brain [12, 13]. These antioxidants, particularly ellagitannins, are naturally-occurring in foods such as berries, nuts, grapes and teas, and have demonstrated preventative effects in animal models of chronic disease, such as cancer, diabetes, cardiovascular, renal and neurodegenerative diseases [12, 14–18]. One of the highest polyphenol-containing dietary supplements available commercially is pomegranate juice (POM), which has been studied *in vitro* and *in vivo* without any side effects [17, 19, 20]. Animal models of hypoxic-ischemic injury have documented its neuroprotectant effects following maternal supplementation [21, 22], with evidence for dose and time-dependent effects [22]. Relatedly, polyphenols have been shown to attenuate oxidative stress and apoptosis in cultured human trophoblasts, implicating a role for p53 downregulation [23, 24]. Collectively, these studies suggest prenatal administration of polyphenols may aid in neuroprotection for infants with hypoxic-ischemic injury.

To date, no human study has investigated maternal polyphenol administration as a neuroprotectant in at-risk newborns. To test if *in utero* administration can protect against hypoxic-ischemia, a model of prenatal brain injury is required. Intrauterine growth restriction (IUGR), defined as growth *in utero* that fails to meet the endogenous potential of the fetus [25, 26], represents one such model. Importantly, fetuses with IUGR often suffer long-term placental insufficiency resulting in chronic hypoxia similar to hypoxic-ischemic injury following acute perinatal injury [27]. Furthermore, the vulnerability of the developing brain in infants with IUGR has been demonstrated in term-equivalent magnetic resonance imaging (MRI) studies [28, 29].

The current exploratory study sought to investigate relationships between maternal POM supplementation and infant brain macrostructure, microstructural organization and functional connectivity in pregnancies with IUGR.

2. Materials and methods

2.1. Trial design and participants

This was a randomized, controlled, double-blind pilot study of maternal POM consumption during pregnancy. The sample was recruited from an inner city US population, with the study conducted at Barnes-Jewish Hospital in St Louis, Missouri during 2012–2014. A study coordinator evaluated expectant mothers receiving prenatal care for enrollment. Inclusion criteria were: 1) fetal diagnosis of IUGR defined by estimated fetal weight <10th percentile for gestational age [25, 26]; 2) 24–34 weeks' gestation based on ultrasound or reliable clinical dating by ACOG standards [30]. Exclusion criteria were: 1) major congenital abnormalities; 2) known fetal chromosomal disorder; 3) maternal illicit drug use; 4) maternal HIV and/or hepatitis C infection; 4) premature rupture of membranes. All protocols were in accordance with the 1964 Helsinki declaration and its amendments or comparable ethical standards. The study was approved by the Washington University Institutional Review Board. Written informed consent was obtained for all participants.

2.2. Initial visit

Sociodemographic, health status and pregnancy information were collected for consented participants by questionnaires. Maternal blood was drawn at enrollment to measure baseline metabolite levels, specifically urolithin A (UA) and dimethylelagic acid glucuronide (DMEAG).

2.3. Randomization

Participants were randomized by a computerized random number generator to treatment or placebo in a 1:1 ratio, and completed either a daily regimen of 8 oz. of 100% pomegranate juice (POM Wonderful, Los Angeles, CA) or a control beverage, respectively. Allocation concealment was achieved using sequentially numbered opaque sealed envelopes generated using a random number generator with each opaque envelope pulled in numerical sequence. Total polyphenols in the beverages were determined by the Folin-Ciocalteu method calibrated by a gallic acid standard curve and reported as gallic acid equivalents (GAE) [20, 31, 32]. Pomegranate juice (16° Brix) contained no less than 700mg GAE. The control beverage (16° Brix) was polyphenol-free (no more than 38 mg GAE), matched for sensory characteristics and calorie content. The juice was labeled A or B such that the investigative team, participants and healthcare providers remained blinded. Participants were instructed to begin juice consumption following initial blood draw at enrollment through delivery.

2.4. Follow-up and compliance

Participants were followed from enrollment until delivery. Participants kept a daily diary documenting the number of days of juice consumption. Maternal and cord blood was collected at delivery and analyzed to determine change in polyphenol levels from baseline and confirm the presence of transferred pomegranate metabolites. Mode of delivery, complications, APGAR scores, weight, head circumference and length were recorded. Clinically-stable infants underwent term-equivalent brain MRI. While formal neurodevelopmental follow up was planned to take place at 18–24 months of age, this was not conducted due to principal investigator relocation and study cessation.

2.5. Image acquisition

Infants were scanned without sedation at 36–41 weeks postmenstrual age on a Siemens Trio 3T scanner (Erlangen, Germany) [33]. Images included T_1 -weighted (TR/TE 1550/3.05 ms, voxel size 1×1×1.3 mm³) and T_2 -weighted (TR/TE 8210/161 ms; voxel size 1×1×1 mm³)

sequences. Diffusion data were obtained using a spin-echo echo-planar-image (EPI) sequence with 27 b values ranging from 0 to 1200 s/mm² and spatial resolution 2×2×2 mm³. A gradient echo, EPI sequence sensitized to T_2^* blood oxygen dependent (BOLD) signal changes (TR/TE 2910/28 ms, voxel size 2.4×2.4×2.4 mm³) was used to collect 200 frames (~10 minutes) of resting state-functional connectivity MRI data (fcMRI). Images were interpreted by pediatric neuroradiologists (Drs. Shimony and McKinstry) and a neonatologist (TEI).

2.6. Image analysis

Brain abnormalities were scored on T_1 - and T_2 -weighted images using the Kidokoro scoring system [34]. Brain metrics were calculated on aligned T_2 -weighted images [35]. Total and regional brain volumes were estimated using MANTiS (S1 Fig) [36]. Diffusion data was processed using a tensor model [37]. Images were registered to an in-house neonatal T_2 atlas and distortion and motion corrected using FSL [38]. Regions of interest (ROIs) were manually drawn on each brain [37] using Analyze (Mayo Clinic, Rochester, MN) in the corpus callosum and bilateral anterior and posterior limbs of the internal capsule (ALIC, PLIC), optic radiations, frontal lobes, cingulum bundle and centrum semiovale, to generate diffusion tensor imaging (DTI) measures of fractional anisotropy (FA), mean (MD), radial (RD) and axial diffusivity (AD). Ten subjects were excluded from DTI analysis due to processing failure (6 control, 4 treatment).

fcMRI data was processed as previously described [39, 40]. Frames with significant motion (>0.5 mm displacement) were excluded [41]; at least 5 minutes of low-motion BOLD data was required for inclusion. Correlation matrices were constructed using 214 cortical and subcortical grey matter ROIs [42–44]. ROI:ROI correlation coefficients were computed using the Pearson product moment formula [45], and Fisher z-transformed [46]. Time series covariance estimates were computed to preserve sensitivity for detecting fcMRI alterations [45, 47]. Composite scores providing mean correlation and covariance within resting state networks (RSN) and between each network pair were computed to reduce data dimensionality and suppress sampling error [48]. Eighteen subjects were excluded from analysis due to no data (5 control, 2 treatment), motion (2 control, 8 treatment) or processing failure (1 treatment).

2.7. Safety assessment

Safety was assessed by analysis of adverse events; laboratory investigations, including assessment of sepsis and necrotizing enterocolitis (NEC), cardiorespiratory complications, and evaluation of intraventricular hemorrhage (IVH) on clinical ultrasound [49]. Assessors were unaware of study-group allocation.

2.8. Outcome measures

Primary outcomes: Term-equivalent MRI measures of brain structure and connectivity included: brain injury, metrics and volumes; ROI measures of FA, MD, AD and RD; and network composite correlation and covariance measures.

Secondary outcomes: Measures of treatment compliance included number of days of juice consumption, maternal blood metabolite concentrations (enrollment and delivery) and cord blood metabolite concentrations. Safety outcomes included NICU and special care nursery admission, and incidences of respiratory distress, resuscitation, IVH, sepsis and NEC.

2.9. Statistical analysis

Analyses were conducted using SAS 9.4 (SAS Institute, Cary, N.C.) and STATA 13.1 (Stata-Corp, Texas, USA). Power calculations were based on effect sizes with regard to the primary

brain outcome measures of a comparable study in high-risk infant populations, which reported standardized effect sizes between 0.7–1.3 [50]. Accounting for the feasibility of our study, 80 subjects (40 per study arm) yields 80% power based on a two-tailed test of significance ($\alpha = 0.05$) to detect effect sizes of at least 0.7.

Modified intention-to-treat (mITT) analyses were conducted including randomized participants who received their allocated intervention and who underwent brain MRI. This mITT design was necessary given the primary outcome measure—MRI measures of brain structure and connectivity—could only be assessed for infants who underwent term-equivalent brain MRI. Per-protocol (PP) analyses were conducted including participants who strictly adhered to the protocol based on metabolite status, i.e. comparing metabolite-positive (UA or DMEAG) treatment participants with metabolite-negative placebo participants. Group differences in brain outcome measures were assessed using generalized linear models adjusted for postmenstrual age at scan, except for brain injury which was assessed using Fisher's exact test for categorical variables due to small cell numbers. Differences in compliance and safety measures were tested using χ^2 or Fisher's exact test for categorical variables and Student *t*-tests for continuous variables. For outcome variables with skewed distributions that were unable to be normalized by transformation, quantile regression was used to estimate the conditional median of the response variable. Due to the exploratory nature of this study, we did not adjust for multiple corrections [51, 52].

3. Results

Eighty eligible mothers were enrolled and randomly assigned to treatment and placebo groups (Fig 1). Two mothers withdrew from the study prior to randomization. One subject was excluded for technical reasons. Following randomization, 6 mothers (7.7%) did not receive the allocated intervention, of whom 3 requested withdrawal (placebo), 1 was excluded due to positive drug screen (treatment) and 2 were excluded due to congenital anomalies (treatment). A total of 34 (91.9%) placebo and 37 (90.2%) treatment subjects were followed to delivery, of whom 27 (79.4%) and 28 (75.7%) underwent term-equivalent MRI, respectively.

3.1. Baseline characteristics and clinical outcomes

The groups were similar in all baseline and demographic characteristics in both mITT and PP analyses, including IUGR severity as indicated by estimated fetal weight and growth percentiles at enrollment and birth weight Z-scores [53] (Table 1). There were no differences in other clinical outcomes between groups except for a modestly lower cord arterial base excess in the treatment group compared with placebo in the PP analysis. There were no differences between participants lost to follow-up ($n = 22$) and those who underwent infant MRI ($n = 55$), except for a greater percentage of preterm infants lost to follow-up (<37 weeks: 13 (59%) v. 12 (23%), $p = 0.002$; <34 weeks: 10 (45%) v. 3 (5%), $p < 0.001$), although this was not associated with treatment arm.

3.2. Brain outcomes

While there was no difference in brain injury (S1 Table), brain metrics (S2 Table) or brain volumes (S3 Table) between treatment and placebo subjects, we observed group differences in DTI measures. Specifically, the treatment group displayed reduced MD compared with placebo in the ALIC, PLIC and centrum semiovale which was mediated by reduced RD (Fig 2A, S4 Table). These differences remained in PP analysis for the left ALIC and right PLIC (Fig 2B, S4 Table). The treatment group also demonstrated increased FA in the right ALIC and right cingulum, although these differences did not remain in PP analysis.

CONSORT
TRANSPARENT REPORTING of TRIALS

CONSORT 2010 Flow Diagram

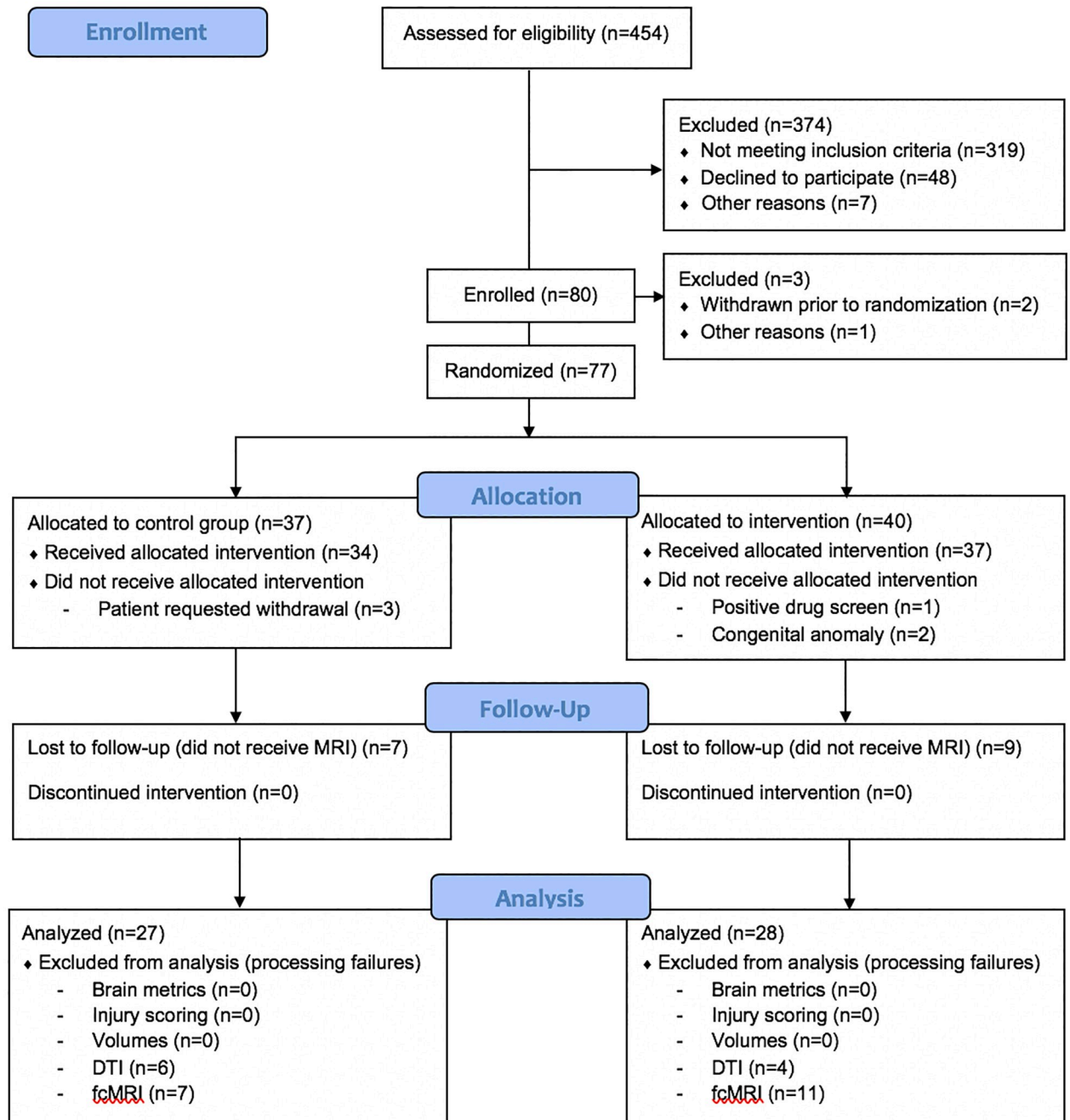


Fig 1. Participant flowchart.

<https://doi.org/10.1371/journal.pone.0219596.g001>

fcMRI correlation and covariance matrices from mITT and PP analyses are shown in Figs 3 and 4. RSNs demonstrating the greatest differences in the treatment group are identifiable in Table 2, S2 and S3 Figs, which include composite mean correlation and covariance measures. In the mITT analysis, there was increased correlation in the subcortical network in treatment compared with placebo subjects (Table 2, Fig 3, S2 Fig). Further, in PP analysis we observed increased fcMRI measures in several networks in metabolite-positive treatment subjects, relative to metabolite-negative controls. Specifically, there was increased correlation within the visual network (Table 2, Fig 3, S2 Fig) and increased covariance within subcortical, visual, salience and default mode networks (Table 2, Fig 4, S3 Fig).

3.3. Compliance

Juice consumption and maternal metabolite presence (either UA or DMEAG present) at enrollment did not differ between groups (Table 3). There was a higher incidence of maternal metabolite presence at delivery in the treatment group than placebo, however, almost one-third of treatment subjects did not have maternal metabolites and almost one-half of placebo subjects had metabolites. Sixty-one percent of treatment and 33% of placebo subjects tested positive for cord blood metabolite presence. To address this variability and allow stricter investigation of relationships between POM intake and brain structure and function, PP analyses were performed using only metabolite-positive treatment, and metabolite-negative placebo subjects (Table 3).

3.4. Safety assessment

There were no group differences with respect to any complications (Table 4). Specifically, there were no complications noted in either group consistent with pulmonary hypertension or any clinical evidence consistent with premature closure of a patent ductus arteriosus (PDA). As no adverse events were found to be attributable to POM, no stopping rules were implemented.

4. Discussion

This is the first study reporting relationships between maternal POM intake and brain structure and function in infants with IUGR. While we did not observe differences in brain macrostructure, we report regional differences in white matter microstructure and functional connectivity in association with POM intake, suggesting potential *in utero* effects on the newborn brain.

The antioxidant effects of POM have been demonstrated *in vitro* and *in vivo* without any proven side effects [17, 19, 20]. Loren *et al.* reported over 60% reduction in brain tissue loss in mice with hypoxic-ischemia born to dams receiving POM [21]. Further, maternal POM supplementation was recently shown to attenuate maternal inflammation-induced rat fetal brain injury [54], and rescue hypoxia-induced fetal growth restriction in pregnant mice [55]. In the current study, the lack of an observable association with brain injury may reflect its low incidence, which necessitated grouping all infants with injury and possibly masked potential benefits in those with milder injury. Indeed, therapeutic hypothermia has shown greater benefits in subjects with less severe injury [56].

Brain metrics have been shown to reliably quantify growth in high-risk infants, such as those born preterm [35, 57]. However, they are only a surrogate measure of brain volume,

Table 1. Baseline characteristics and clinical outcomes of study participants.

Variable	MODIFIED INTENTION-TO-TREAT		PER-PROTOCOL	
	Placebo (n = 27)	POM (n = 28)	Placebo, Metabolite-ve (n = 15)	POM, Metabolite +ve (n = 17)
<i>Baseline Characteristics</i>				
Maternal age (years), mean (SD)	26.9 (6.7)	24.4 (6.1)	25.9 (7.3)	24.7 (6.9)
Race, Black, n (%)	17 (63)	21 (75)	9 (60)	12 (71)
Race, White, n (%)	8 (30)	7 (25)	5 (33)	5 (29)
Smoking, n (%)	7 (26)	7 (25)	5 (33)	4 (24)
Substance use, n (%)	0 (0)	0 (0)	0 (0)	0 (0)
Sickle cell disease, n (%)	0 (0)	0 (0)	0 (0)	0 (0)
Gestational age at enrollment, mean (SD)	30.5 (2.6)	30.8 (2.5)	30.4 (2.8)	30.8 (2.6)
Gestational age at enrollment, median (IQR)	31 (28, 33)	31.5 (29, 32.5)	31 (28, 33)	32 (29, 33)
Estimated fetal weight at enrollment (g), mean (SD)	1187.3 (374.8)	1194.5 (380.0)	1205.7 (414.2)	1184.6 (428.9)
Growth percentile at enrollment, mean (SD)	6.8 (2.0)	6.0 (2.1)	7.3 (2.1)	6.5 (2.2)
Steroids for fetal lung maturity, n (%)	1 (4)	2 (7)	0 (0)	1 (6)
<i>Maternal & Delivery Outcomes</i>				
Gestational age at delivery, weeks, mean (SD)	37.4 (1.6)	36.8 (2.5)	36.9 (1.7)	37.1 (2.0)
PMA at MRI scan, weeks, mean (SD)	38.6 (1.3)	38.3 (1.6)	38.2 (1.2)	38.1 (1.5)
Preterm birth <37 weeks, n (%)	4 (15)	7 (25)	3 (20)	4 (24)
Preterm birth <34 weeks, n (%)	0 (0)	3 (11)	0 (0)	2 (12)
Mode of delivery (vaginal), n (%)	18 (67)	19 (68)	12 (80)	13 (76)
Meconium stained amniotic fluid, n (%)	1 (4)	1 (4)	1 (7)	1 (6)
<i>Neonatal Outcomes</i>				
Sex, n (%)	13 (48)	13 (46)	8 (53)	8 (47)
Birthweight (g), mean (SD)	2536.6 (367.5)	2385.2 (476.7)	2344.7 (289.7)	2415.9 (378.8)
Birthweight Z-score, mean (SD)	-1.03 (0.70)	-1.09 (0.55)	-1.23 (0.78)	-1.10 (0.57)
APGAR score at 1 minute, median (IQR)	8 (8, 9)	8 (8, 8)	8 (7, 8)	8 (8, 8)
APGAR score at 5 minutes, median (IQR)	9 (9, 9)	9 (8.5, 9)	9 (9, 9)	9 (9, 9)
Cord arterial pH, mean (SD)	7.29 (0.05)	7.27 (0.05)	7.30 (0.05)	7.26 (0.05)
Cord arterial base excess, mean (SD)	-2.55 (1.69)	-2.97 (1.25)	-2.54 (1.40)	-3.00 (1.34)
Respiratory distress syndrome, n (%)	5 (19)	6 (21)	3 (20)	1 (6)
Variable	MODIFIED INTENTION-TO-TREAT		PER-PROTOCOL	
	Placebo (n = 27)	POM (n = 28)	Placebo, Metabolite-ve (n = 15)	POM, Metabolite +ve (n = 17)
<i>Baseline Characteristics</i>				
Maternal age (years), mean (SD)	26.9 (6.7)	24.4 (6.1)	25.9 (7.3)	24.7 (6.9)
Race, Black, n (%)	17 (63)	21 (75)	9 (60)	12 (71)
Race, White, n (%)	8 (30)	7 (25)	5 (33)	5 (29)
Smoking, n (%)	7 (26)	7 (25)	5 (33)	4 (24)
Substance use, n (%)	0 (0)	0 (0)	0 (0)	0 (0)
Sickle cell disease, n (%)	0 (0)	0 (0)	0 (0)	0 (0)
Gestational age at enrollment, mean (SD)	30.5 (2.6)	30.8 (2.5)	30.4 (2.8)	30.8 (2.6)
Gestational age at enrollment, median (IQR)	31 (28, 33)	31.5 (29, 32.5)	31 (28, 33)	32 (29, 33)
Estimated fetal weight at enrollment (g), mean (SD)	1187.3 (374.8)	1194.5 (380.0)	1205.7 (414.2)	1184.6 (428.9)
Growth percentile at enrollment, mean (SD)	6.8 (2.0)	6.0 (2.1)	7.3 (2.1)	6.5 (2.2)
Steroids for fetal lung maturity, n (%)	1 (4)	2 (7)	0 (0)	1 (6)
<i>Maternal & Delivery Outcomes</i>				
Gestational age at delivery, weeks, mean (SD)	37.4 (1.6)	36.8 (2.5)	36.9 (1.7)	37.1 (2.0)
PMA at MRI scan, weeks, mean (SD)	38.6 (1.3)	38.3 (1.6)	38.2 (1.2)	38.1 (1.5)

(Continued)

Table 1. (Continued)

Preterm birth <37 weeks, <i>n</i> (%)	4 (15)	7 (25)	3 (20)	4 (24)
Preterm birth <34 weeks, <i>n</i> (%)	0 (0)	3 (11)	0 (0)	2 (12)
Mode of delivery (vaginal), <i>n</i> (%)	18 (67)	19 (68)	12 (80)	13 (76)
Meconium stained amniotic fluid, <i>n</i> (%)	1 (4)	1 (4)	1 (7)	1 (6)
<i>Neonatal Outcomes</i>				
Sex, <i>n</i> (%)	13 (48)	13 (46)	8 (53)	8 (47)
Birthweight (g), mean (SD)	2536.6 (367.5)	2385.2 (476.7)	2344.7 (289.7)	2415.9 (378.8)
Birthweight Z-score, mean (SD)	-1.03 (0.70)	-1.09 (0.55)	-1.23 (0.78)	-1.10 (0.57)
APGAR score at 1 minute, median (IQR)	8 (8, 9)	8 (8, 8)	8 (7, 8)	8 (8, 8)
APGAR score at 5 minutes, median (IQR)	9 (9, 9)	9 (8.5, 9)	9 (9, 9)	9 (9, 9)
Cord arterial pH, mean (SD)	7.29 (0.05)	7.27 (0.05)	7.30 (0.05)	7.26 (0.05)
Cord arterial base excess, mean (SD)	-2.55 (1.69)	-2.97 (1.25)	-2.54 (1.40)	-3.00 (1.34)
Respiratory distress syndrome, <i>n</i> (%)	5 (19)	6 (21)	3 (20)	1 (6)

BMI—body mass index; IQR—interquartile range; POM—pomegranate; PMA—postmenstrual age; SD—standard deviation

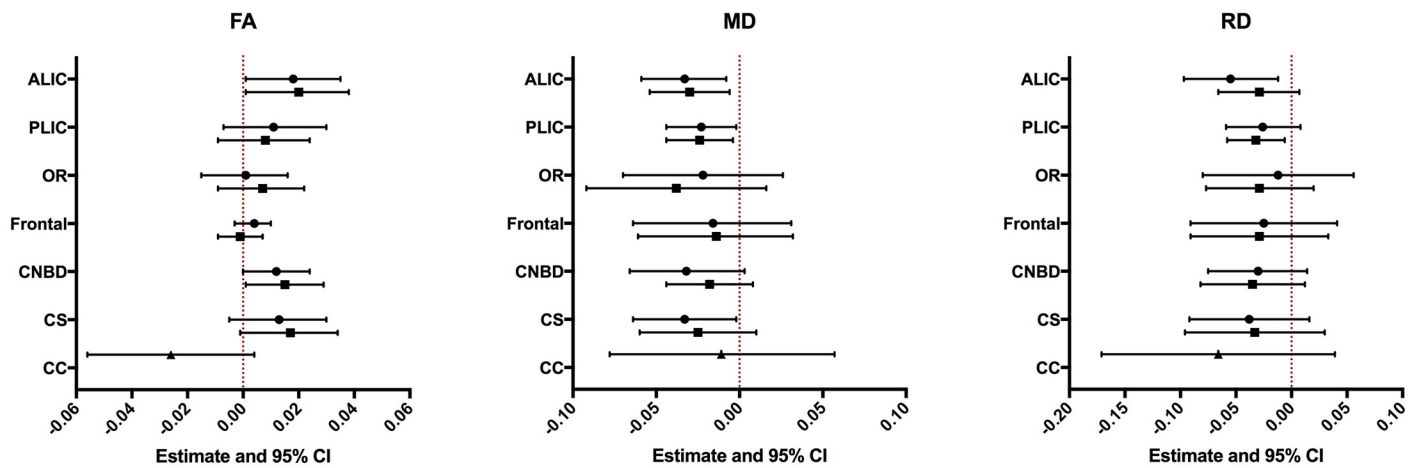
<https://doi.org/10.1371/journal.pone.0219596.t001>

with limited sensitivity for detecting group differences in small samples. Volumetric analyses have demonstrated regional vulnerabilities within the hippocampus, brainstem and thalamus, and the watershed zone in term newborns with hypoxic-ischemic injury [58, 59]. The existence of corresponding regional neuroprotective effects of polyphenols remains unclear. While we were likely underpowered to detect such effects, animal studies have reported protective effects in hippocampal and cortical regions [21, 60–69].

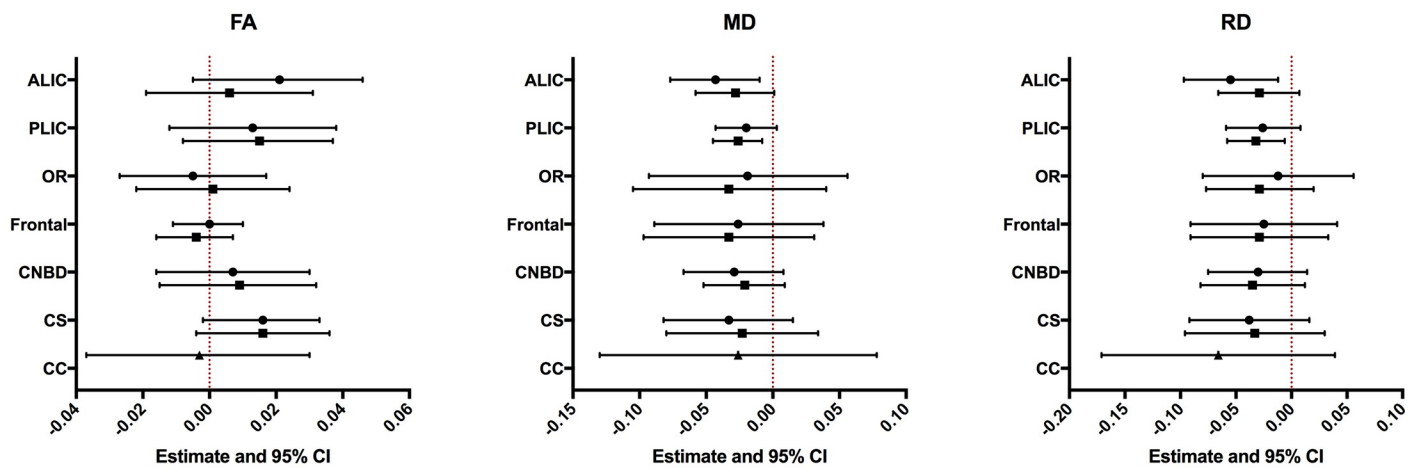
It is plausible that responses to POM are partially mediated via mechanisms below the macrostructural level. DTI investigations offer a complementary approach to conventional MRI, providing added insight regarding microscopic white matter organization. Here, we observed regional microstructural alterations in association with maternal POM intake, implicating the ALIC and PLIC, cingulum and centrum semiovale; areas previously shown to be vulnerable to the effects of hypoxic-ischemia [58, 70]. These findings were present in both mITT and PP analyses. While definitive interpretation of DTI changes remains complicated [71, 72], increased FA is observed in more mature white matter [73], while reduced FA likely reflects axonal damage, reduced myelination and/or reduced neuroglial packing density [74, 75], and is often reported in very preterm infants (VPT) relative to term born peers [76]. MD is a summary measure of diffusivity, with increased values reflecting immature, poorly developed white matter [75, 77], as often seen in VPT infants compared with full term peers [76]. AD and RD provide complementary information; the former reflecting axonal organization and density, with RD reflecting alterations in myelination [75, 78]. Thus, we postulate *in utero* POM exposure may lead to improved maturation, via neuroprotective mechanisms such as axonal sparing and/or remyelination. This appears to be supported by evidence of improved motor function in association with pomegranate supplementation in mice models of cytotoxic radiation [79], and cognitive and behavioral improvements in mouse models of Alzheimer's [80], implicating a role for enhanced synaptic plasticity [81].

In utero POM exposure may also lead to changes in functional networks in the developing brain. fMRI delineates the brain's functional architecture, including widely-distributed, cortically-based RSNs known to be co-activated by task [82], several of which have been described in infants [39, 47]. In the current study, metabolite-positive treatment subjects displayed increased connectivity, characterized by greater correlation and covariance, within visual, subcortical, salience and default mode networks. Consistent with previous reports, covariance was

MODIFIED INTENTION-TO-TREAT



PER-PROTOCOL



● Left ■ Right

Fig 2. Relationships between maternal pomegranate juice intake and infant DTI measures. (Top) Treatment vs. placebo (modified intention-to-treat analysis). (Bottom) Metabolite-positive treatment vs. metabolite-negative placebo (per-protocol analysis). The point estimates represent the difference between groups in white matter DTI measures based on analyses run using generalized linear models (GLM) adjusted for postmenstrual age at scan. The error bars represent the 95% confidence intervals. ALIC—anterior limb of internal capsule; CC—corpus callosum; CNBD—cingulum bundle; CSOV—centrum semiovale; FA—fractional anisotropy; Frontal—frontal lobe; OR—optic radiation; MD—mean diffusivity; PLIC—posterior limb of internal capsule; RD—radial diffusivity. Left/Right indicate measures for bilateral white matter tracts.

<https://doi.org/10.1371/journal.pone.0219596.g002>

more sensitive to these alterations than correlation measures [45]. Of note, the most apparent alterations were observed in the visual cortex, an early maturing, developmentally vulnerable cortical region [83, 84]. Interestingly, these findings survived supplemental analyses correcting for multiple comparisons using the false discovery rate [85]. The retina has been increasingly shown to be susceptible to the effects of hypoxic-ischemia [86, 87], with mechanisms involving glutamate excitotoxicity and oxidative glutamate toxicity implicated [88, 89]. Furthermore, studies have demonstrated the therapeutic potential of polyphenols in reducing oxidative stress-induced death of retinal ganglion and pigment epithelial cells [90–93].

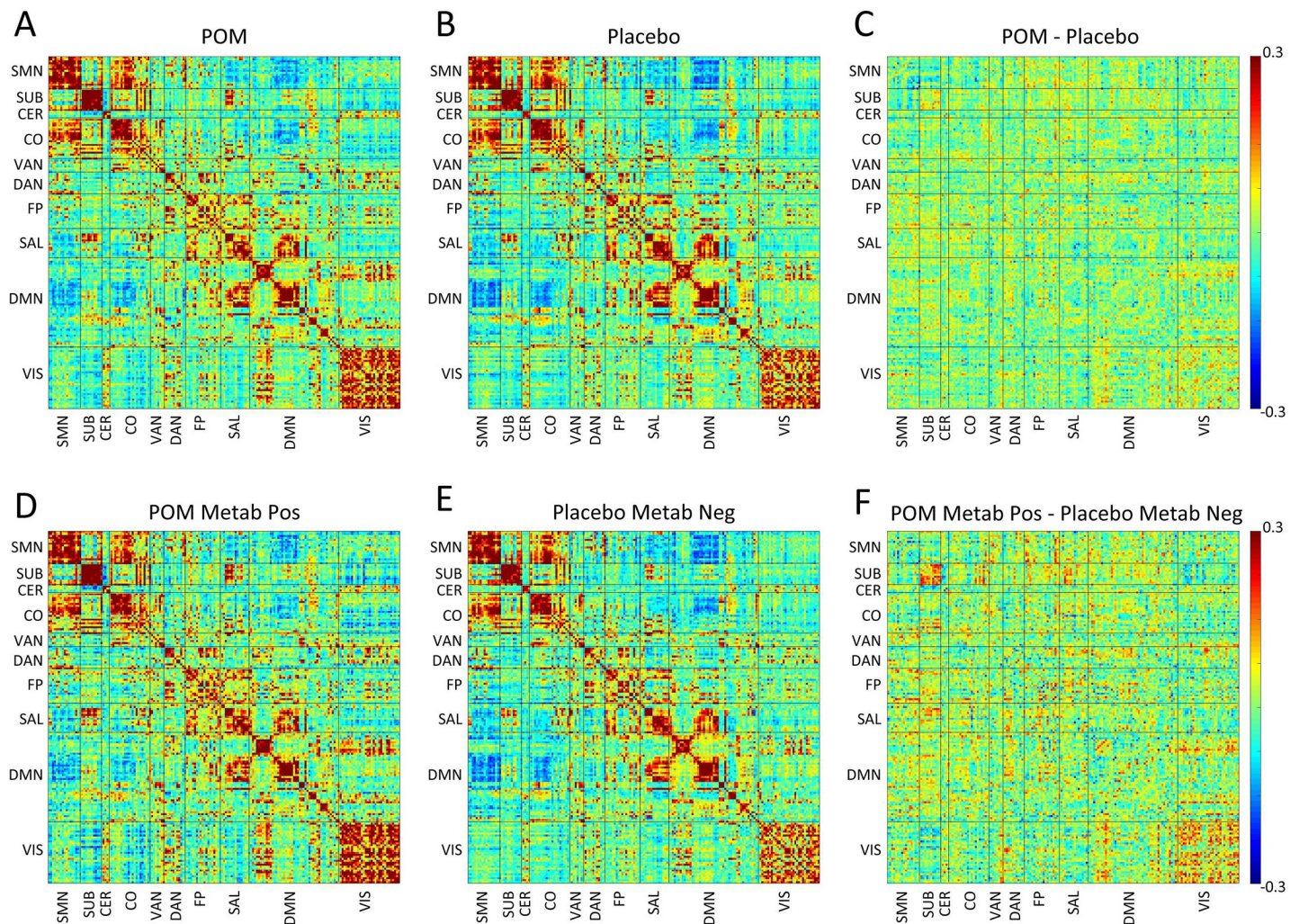


Fig 3. Relationships between maternal pomegranate juice intake and infant fMRI measures (correlations). Group mean Fisher’s z-transformed correlation coefficient matrices are shown representing all ROI pairs. The block structure along the diagonal seen in both groups corresponds to resting state networks. Warm hues within diagonal blocks reflect positively correlated ROIs within RSN, while cool hues reflect negatively correlated ROIs within RSNs. (Top, A-C) Treatment vs. placebo (modified intention-to-treat analysis). (A) Infants in treatment (pomegranate juice) group and (B) infants in placebo group at term-equivalent. (C) Shows the difference between groups (treatment minus placebo). (Bottom, D-F) Metabolite-positive treatment vs. metabolite-negative placebo (per-protocol analysis). (D) Infants in metabolite-positive treatment group and (E) infants in metabolite-negative placebo group at term-equivalent. (F) Shows the difference between groups (metabolite-positive treatment minus metabolite-negative placebo). Note metabolite-positive treatment > metabolite-negative placebo correlation in subcortical and visual network. CER—cerebellar; CO—cingulo-opercular; DAN—dorsal attention network; DMN—default mode network; FP—frontal parietal network; LAN—language area network; Metab—metabolite; Neg—negative; POM—pomegranate; Pos—positive; SAL—salience network; SMN—sensorimotor network; SUB—subcortical grey matter; VAN—ventral attention network; VIS—visual network.

<https://doi.org/10.1371/journal.pone.0219596.g003>

Of note, there was little evidence for microstructural changes within corresponding white matter tracts such as the optic radiations. While some studies demonstrate robust relationships between DTI and fMRI findings [94, 95], others have not [96–98], suggesting that structural and functional connectivity may not interrelate via a one-to-one relationship. Future studies combining these modalities are likely to improve our understanding of structure–function interactions in the developing brain. It is worth noting that the observed microstructural and functional connectivity alterations may be related to later neurodevelopmental outcomes; investigations are currently underway to better understand these relationships. Further, though the current study employed term-equivalent MRI, investigations including fetal MRI may provide additional insight into brain development trajectories following *in utero* POM exposure.

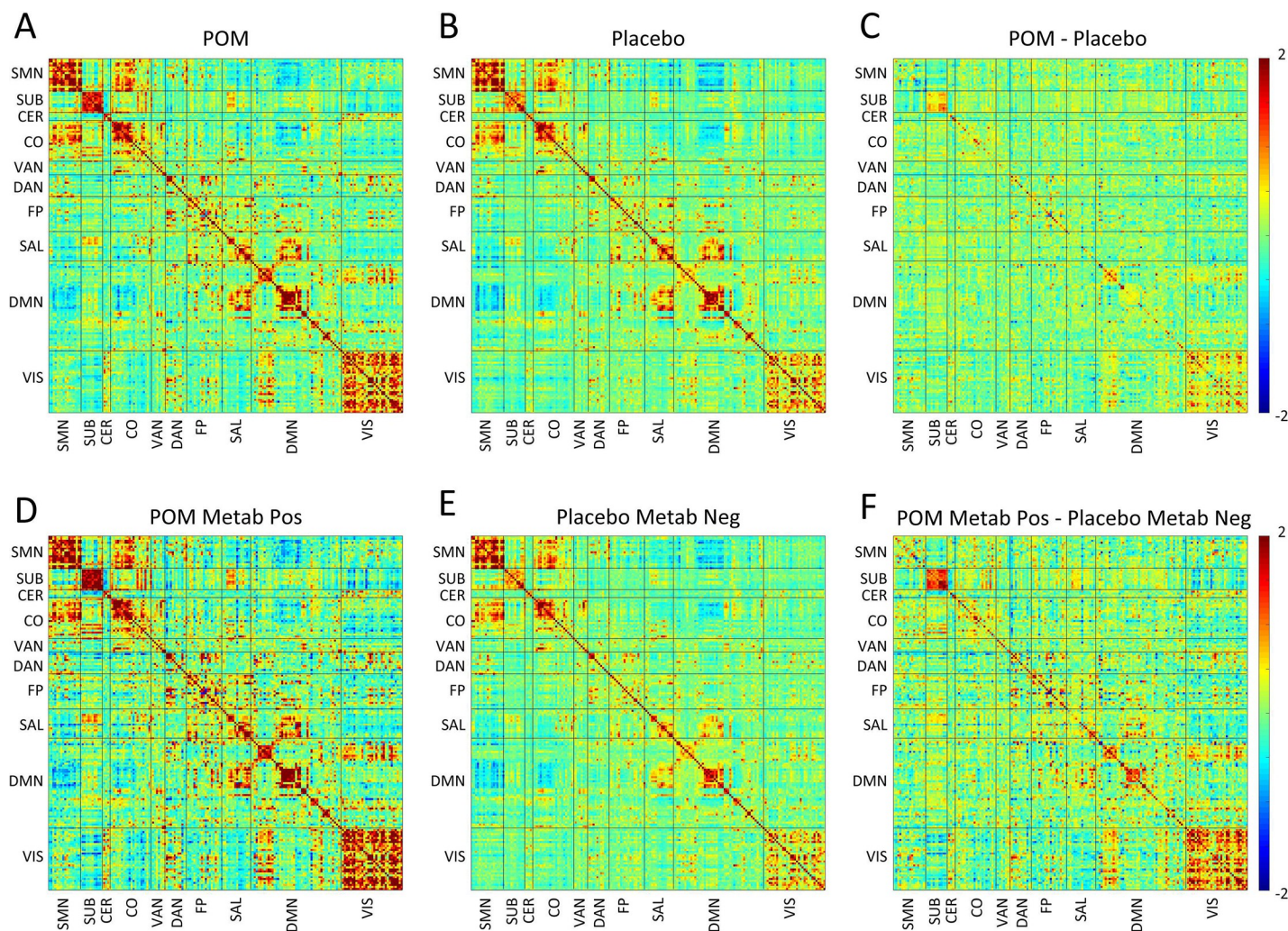


Fig 4. Relationships between maternal pomegranate juice intake and infant fMRI measures (covariance). Group mean covariance matrices are shown representing all ROI pairs. The block structure along the diagonal seen in both groups corresponds to resting state networks. Warm hues within diagonal blocks reflect positively correlated ROIs within RSN, while cool hues reflect negatively correlated ROIs within RSNs. (Top, A-C) Treatment vs. placebo (modified intention-to-treat analysis). (A) Infants in treatment (pomegranate juice) group and (B) infants in placebo group at term-equivalent. (C) Shows the difference between groups (treatment minus placebo). Note treatment > placebo covariance within subcortical and visual networks. (Bottom, D-F) Metabolite-positive treatment vs. metabolite-negative placebo (per-protocol analysis). (D) Infants in metabolite-positive treatment group and (E) infants in metabolite-negative placebo group at term-equivalent. (F) Shows the difference between groups (metabolite-positive treatment minus metabolite-negative placebo). Note metabolite-positive treatment > metabolite-negative placebo covariance within subcortical and visual networks. CER—cerebellar; CO—cingulo-opercular; DAN—dorsal attention network; DMN—default mode network; FP—frontal parietal network; LAN—language area network; Metab—metabolite; Neg—negative; POM—pomegranate; Pos—positive; SAL—salience network; SMN—sensorimotor network; SUB—subcortical grey matter; VAN—ventral attention network; VIS—visual network.

<https://doi.org/10.1371/journal.pone.0219596.g004>

The current study supports the therapeutic potential of polyphenols such as POM for hypoxic-ischemic injury, however, our findings need to be considered with respect to several limitations. In the current study consumption of 8 oz. POM provided a daily administration of no less than 700 mg GAE of polyphenols [20]. Ellagitannins are metabolized by colonic gut microbiota to generate more readily absorbed metabolites, specifically UA and DMEAG [99–101], proposed to be the bioactive molecules underlying the neuroprotectant effects of POM [99–102]. However, there are challenges associated with the chemical estimation methods employed to assess metabolite bioavailability [60], further compounded by intra-subject variability in polyphenol metabolism arising from genetic polymorphisms in metabolizing

Table 2. Composite mean Fisher z-transformed correlations and mean covariance by group status, adjusted for postmenstrual age at scan.

	Group Summaries								Group Comparisons ¹							
	POM (n = 17)		POM, Metabolite +ve (n = 10)		Placebo (n = 20)		Placebo, Metabolite -ve (n = 14)		MODIFIED INTENTION-TO-TREAT				PER-PROTOCOL			
Network correlation	Mean	SD	Mean	SD	Mean	SD	Mean	SD	Estimate	SE	t	P	Estimate	SE	t	P
SMN	0.26	0.06	0.26	0.07	0.28	0.05	0.28	0.06	-0.02	0.02	-1.04	0.30	-0.02	0.03	-0.57	0.57
SUB ²	0.41		0.42		0.34		0.33		0.09	0.04	2.23	0.03	0.11	0.08	1.45	0.15
CER	0.25	0.14	0.22	0.11	0.22	0.10	0.22	0.10	0.04	0.04	0.89	0.38	0.00	0.04	-0.05	0.96
CO ²	0.18		0.18		0.17		0.15		-0.005	0.02	-0.21	0.84	0.02	0.03	0.71	0.48
VAN	0.13	0.04	0.14	0.03	0.12	0.05	0.11	0.05	0.01	0.02	0.89	0.38	0.03	0.02	1.47	0.16
DAN	0.12	0.06	0.12	0.07	0.11	0.05	0.12	0.05	0.00	0.02	0.04	0.97	0.00	0.02	0.14	0.89
FP	0.14	0.05	0.15	0.06	0.12	0.04	0.13	0.04	0.01	0.01	0.68	0.50	0.02	0.02	0.86	0.40
SAL	0.17	0.05	0.19	0.04	0.18	0.07	0.16	0.06	-0.01	0.02	-0.57	0.57	0.02	0.02	1.04	0.31
DMN	0.08	0.02	0.08	0.03	0.07	0.02	0.07	0.02	0.00	0.01	0.20	0.84	0.00	0.01	0.34	0.74
VIS	0.22	0.08	0.25	0.07	0.19	0.08	0.16	0.07	0.04	0.03	1.34	0.19	0.09	0.03	2.87	0.01
Network covariance	Mean	SD	Mean	SD	Mean	SD	Mean	SD	Estimate	SE	t	P	Estimate	SE	t	P
SMN ²	1.30		1.51		1.33		1.28		-0.09	0.15	-0.61	0.55	0.12	0.19	0.61	0.55
SUB ²	0.97		1.05		0.84		0.80		0.29	0.24	1.21	0.24	0.72	0.30	2.40	0.03
CER ²	0.85		0.86		0.55		0.55		0.15	0.10	1.41	0.17	0.13	0.13	1.01	0.32
CO ²	0.70		0.81		0.47		0.43		0.15	0.19	0.78	0.44	0.44	0.23	1.92	0.07
VAN ³	0.38		0.50		0.26		0.24		0.10	0.07	1.48	0.15	0.26	0.13	2.01	0.06
DAN ²	0.34		0.47		0.30		0.27		0.20	0.24	0.83	0.41	0.46	0.31	1.46	0.16
FP ²	0.45		0.50		0.30		0.28		0.14	0.09	1.57	0.13	0.20	0.13	1.48	0.15
SAL ²	0.43		0.62		0.35		0.26		0.10	0.24	0.40	0.69	0.68	0.23	2.97	0.01
DMN ²	0.20		0.32		0.20		0.17		0.21	0.18	1.18	0.25	0.55	0.21	2.61	0.02
VIS ²	0.73		1.09		0.45		0.33		0.41	0.26	1.58	0.12	0.99	0.32	3.10	0.01

CER—cerebellar; CO—cingulo-opercular; DAN—dorsal attention network; DMN—default mode network; FP—frontal parietal network; LAN—language area network; POM—pomegranate; SAL—salience network; SMN—sensorimotor network; SUB—subcortical grey matter; VAN—ventral attention network; VIS—visual network

¹ Analyses run using generalized linear models (GLM) adjusted for postmenstrual age at scan

² Distribution skewed (> |0.8|). Analyses run using ln transformed variables (for CER_avg_covariance transformation based on raw value + 1 to account for negative values). Group summary values reflect medians, not means, of the raw distribution

³ Remained skewed after transformation. Raw variable modeled using quantile (median) regression (SAS PROC QUANTREG); group summary values reflect medians, not means, of the distribution

<https://doi.org/10.1371/journal.pone.0219596.t002>

enzymes [100] as well as variations in gut microbiota [103]. There is also limited information on, and variability in, polyphenol content in various food items [60, 104, 105]. While we did not capture information on participant diet, it is reasonable to assume that residual polyphenol-intake from non-pomegranate dietary sources was randomly distributed among study participants given UA and DMEAG were largely absent in both groups at enrolment. Nonetheless, in PP analyses using metabolite positivity as a proxy for polyphenol intake, confounding arising from these factors cannot be excluded. Finally, we did not undertake echocardiography for evaluation of the PDA but there was no clinical evidence seen of premature closure or constriction of the PDA. Direct effects on health were not found.

5. Conclusion

We provide preliminary evidence supporting potential *in utero* effects of POM exposure. Specifically, we report differences suggestive of enhanced microstructural organization within the

Table 3. Measures of compliance.

	MODIFIED INTENTION-TO-TREAT							PER-PROTOCOL						
	Placebo (n = 27)	POM (n = 28)	Absolute Effect Size ¹	Relative Effect Size ²	SE ²	t/ χ^2	P ³	Placebo, Metabolite -ve (n = 15)	POM, Metabolite +ve (n = 17)	Absolute Effect Size ¹	Relative Effect Size ²	SE ²	t/ χ^2	P ³
Days of consumption, median (IQR)	23 (14, 40)	18.5 (7, 30.5)	6.8	0.44	4.17	1.6	0.11	23 (15, 40)	18 (7, 24)	9.7	0.71	4.89	2.0	0.06
Maternal UA or DMEAG at enrollment, n (%)	3 (11)	2 (8) ^a	-3.1%	0.64	0.08		1.00	1 (7)	1 (7)	0.0%	1.00	0.14		1.00
Maternal UA or DMEAG at delivery, n (%)	11 (42) ^b	17 (68) ^c	25.7%	1.49	0.13	3.4	0.07	0 (0)	17 (100)	100.0%	31.11	0.17		<0.001
Cord UA or DMEAG at delivery, n (%)	8 (33) ^d	14 (61) ^e	27.5%	1.69	0.13	3.6	0.06	0 (0)	14 (93)	93.3%	25.78	0.17		<0.001
Positive for metabolites in cord blood or maternal blood at delivery	11 (42) ^f	17 (68) ^g	25.7%	1.49	0.13	3.4	0.07	0 (0)	17 (100)	100.0%	31.11	0.17		<0.001

DMEAG; dimethylglucuronic acid glucuronid; IQR—interquartile range; POM—pomegranate; SE—standard error; UA—uroolithin A

¹ Absolute effect size calculated as the mean difference for continuous variables, and the risk difference (%) for categorical variables (Placebo = reference)

² Relative effect size calculated as Cohen’s *d* for continuous variables, and the relative risk for categorical variables (Placebo = reference). For analyses with zero in one or more cells, 0.5 was added to each cell prior to calculation of the relative risk and its standard error (SE). Corresponding SE are reported.

³ Fisher’s exact test (2-sided) used to compare proportions by group where expected cell size < 5.

^a n = 25

^b n = 26

^c n = 25

^d n = 24

^e n = 23

^f n = 26

^g n = 25

<https://doi.org/10.1371/journal.pone.0219596.t003>

Table 4. Safety assessment.

Complication	Placebo (n = 34)	POM (n = 37)	Risk Difference ¹ (%)	Relative Risk ²	SE ²	χ^2	P ³
NICU admission, n (%)	1 (3)	3 (8)	5.1	2.76	0.05		0.62
Special care nursery admission, n (%)	10 (29)	10 (27)	-2.4	0.92	0.11	0.05	0.82
Respiratory distress, n (%)	7 (21)	9 (24)	3.7	1.18	0.10	0.14	0.71
Resuscitation at delivery, n (%)	5 (15)	8 (22)	6.9	1.47	0.09	0.57	0.45
Intraventricular hemorrhage, n (%)	0 (0)	0 (0)	0.0	-	-	NA	NA
Sepsis, n (%)	2 (0)	1 (3)	-3.2	0.46	0.05		1.00
Necrotizing enterocolitis, n (%)	0 (0)	0 (0)	0	-	-	NA	NA

NICU—neonatal intensive care; POM—pomegranate; SE—standard error

¹ Absolute effect size calculated as the mean difference for continuous variables, and the risk difference (%) for categorical variables (Placebo = reference)

² Relative effect size calculated as Cohen’s *d* for continuous variables, and the relative risk for categorical variables (Placebo = reference). For analyses with zero in one or more cells, 0.5 was added to each cell prior to calculation of the relative risk and its standard error (SE). Corresponding SE are reported.

³ Fisher’s exact test (2-sided) used to compare proportions by group where expected cell size < 5.

<https://doi.org/10.1371/journal.pone.0219596.t004>

ALIC and PLIC and functional connectivity within the visual network. This study provides a foundation for building an evidence base for potential neuroprotective agents that may be effective in the general population of at-risk newborns, such as those with hypoxic-ischemic injury. Importantly, our findings warrant the need for a larger, rigorously designed clinical trial to allow continued investigation into the potential region-specific neuroprotective effects of polyphenols.

Supporting information

S1 Checklist. CONSORT checklist.

(DOC)

S1 Fig. Brain volumetry using MANTiS segmentation in a representative subject.

Red = cortical grey matter; green = white matter; yellow = deep grey matter; grey = cerebellum; purple = brainstem; blue = cerebrospinal fluid; cyan = amygdala.

(PDF)

S2 Fig. Relationships between maternal pomegranate juice intake and infant fcMRI measures (network average correlations).

Composite mean Fisher's z-transformed correlation matrices are shown representing averages over ROI pairs within each network (*Top, A-C*) Treatment vs. placebo (intention-to-treat analysis). (A) Infants in treatment (pomegranate juice) group and (B) infants in placebo group at term-equivalent. (C) Shows the difference between groups (treatment minus placebo). (*Bottom, D-F*) Metabolite-positive treatment vs. metabolite-negative placebo (per-protocol analysis). (D) Infants in metabolite-positive treatment group and (E) infants in metabolite-negative placebo group at term-equivalent. (F) Shows the difference between groups (metabolite-positive treatment minus metabolite-negative placebo). Note metabolite-positive treatment > metabolite-negative placebo network average correlation in subcortical and visual network. CER—cerebellar; CO—cingulo-opercular; DAN—dorsal attention network; DMN—default mode network; FP—frontal parietal network; LAN—language area network; Metab—metabolite; Neg—negative; POM—pomegranate; Pos—positive; SAL—salience network; SMN—sensorimotor network; SUB—subcortical grey matter; VAN—ventral attention network; VIS—visual network.

(PDF)

S3 Fig. Relationships between maternal pomegranate juice intake and infant fcMRI measures (network average covariance).

Composite mean covariance matrices are shown representing averages over ROI pairs within each network (*Top, A-C*) Treatment vs. placebo (modified intention-to-treat analysis). (A) Infants in treatment (pomegranate juice) group and (B) infants in placebo group at term-equivalent. (C) Shows the difference between groups (treatment minus placebo). (*Bottom, D-F*) Metabolite-positive treatment vs. metabolite-negative placebo (per-protocol analysis). (D) Infants in metabolite-positive treatment group and (E) infants in metabolite-negative placebo group at term-equivalent. (F) Shows the difference between groups (metabolite-positive treatment minus metabolite-negative placebo). Note metabolite-positive treatment > metabolite-negative placebo network average covariance within subcortical and visual networks. CER—cerebellar; CO—cingulo-opercular; DAN—dorsal attention network; DMN—default mode network; FP—frontal parietal network; LAN—language area network; Metab—metabolite; Neg—negative; POM—pomegranate; Pos—positive; SAL—salience network; SMN—sensorimotor network; SUB—subcortical grey matter; VAN—ventral attention network; VIS—visual network.

(PDF)

S1 Table. Brain injury by group status, adjusted for postmenstrual age at scan.
(DOCX)

S2 Table. Brain metrics by group status, adjusted for postmenstrual age at scan.
(DOCX)

S3 Table. Brain volumes by group status, adjusted for postmenstrual age at scan.
(DOCX)

S4 Table. DTI measures by group status, adjusted for postmenstrual age at scan.
(DOCX)

S1 File. Study protocol.
(DOC)

Acknowledgments

The authors wish to acknowledge Drs. Joshua Shimony and Robert McKinstry for clinical interpretation of MRI images; Candice Woolfolk for her assistance; as well as the mothers and infants whose time and efforts allow these scientific insights.

Author Contributions

Conceptualization: Christopher D. Smyser, D. Michael Nelson, Terrie E. Inder.

Data curation: Lillian G. Matthews, Sara Cherkerzian, Dimitrios Alexopoulos, Jeanette Kenley, Methodius G. Tuuli, D. Michael Nelson.

Formal analysis: Lillian G. Matthews, Sara Cherkerzian, Dimitrios Alexopoulos, Jeanette Kenley.

Funding acquisition: Christopher D. Smyser, D. Michael Nelson, Terrie E. Inder.

Investigation: Lillian G. Matthews, Christopher D. Smyser, Dimitrios Alexopoulos, Methodius G. Tuuli, D. Michael Nelson, Terrie E. Inder.

Methodology: Lillian G. Matthews, Christopher D. Smyser, Dimitrios Alexopoulos, Jeanette Kenley, Methodius G. Tuuli, D. Michael Nelson, Terrie E. Inder.

Project administration: Lillian G. Matthews, Methodius G. Tuuli.

Resources: Christopher D. Smyser, D. Michael Nelson, Terrie E. Inder.

Software: Lillian G. Matthews, Christopher D. Smyser, Dimitrios Alexopoulos.

Supervision: Christopher D. Smyser, D. Michael Nelson, Terrie E. Inder.

Writing – original draft: Lillian G. Matthews.

Writing – review & editing: Lillian G. Matthews, Christopher D. Smyser, Sara Cherkerzian, Dimitrios Alexopoulos, Jeanette Kenley, Methodius G. Tuuli, D. Michael Nelson, Terrie E. Inder.

References

1. Volpe JJ. Chapter 19. Hypoxic-Ischemic Injury in the Term Infant: Pathophysiology. *Volpe's Neurology of the Newborn*, 6th Edition. 5th ed ed. Philadelphia: Elsevier; 2018. p. 423.
2. Kurinczuk JJ, White-Koning M, Badawi N. Epidemiology of neonatal encephalopathy and hypoxic-ischaemic encephalopathy. *Early human development*. 2010; 86(6):329–38. <https://doi.org/10.1016/j.earlhumdev.2010.05.010> PMID: 20554402

3. Lawn JE, Cousens S, Zupan J. 4 million neonatal deaths: when? Where? Why? *Lancet* (London, England). 2005; 365(9462):891–900.
4. Groenendaal F, Casaer A, Dijkman KP, Gavilanes AWD, de Haan TR, ter Horst HJ, et al. Introduction of Hypothermia for Neonates with Perinatal Asphyxia in the Netherlands and Flanders. *Neonatology*. 2013; 104(1):15–21. <https://doi.org/10.1159/000348823> PMID: 23615314
5. Shah PS, Beyene J, To T, Ohlsson A, Perlman M. Postasphyxial hypoxic-ischemic encephalopathy in neonates: outcome prediction rule within 4 hours of birth. *Archives of pediatrics & adolescent medicine*. 2006; 160(7):729–36.
6. Tekgul H, Gauvreau K, Soul J, Murphy L, Robertson R, Stewart J, et al. The current etiologic profile and neurodevelopmental outcome of seizures in term newborn infants. *Pediatrics*. 2006; 117(4):1270–80. <https://doi.org/10.1542/peds.2005-1178> PMID: 16585324
7. Kumar A, Ramakrishna SV, Basu S, Rao GR. Oxidative stress in perinatal asphyxia. *Pediatric neurology*. 2008; 38(3):181–5. <https://doi.org/10.1016/j.pediatrneurol.2007.10.008> PMID: 18279752
8. Zhao M, Zhu P, Fujino M, Zhuang J, Guo H, Sheikh I, et al. Oxidative Stress in Hypoxic-Ischemic Encephalopathy: Molecular Mechanisms and Therapeutic Strategies. *International Journal of Molecular Sciences*. 2016; 17(12):2078.
9. Ferriero DM. The Vulnerable Newborn Brain: Imaging Patterns of Acquired Perinatal Injury. *Neonatology*. 2016; 109(4):345–51. <https://doi.org/10.1159/000444896> PMID: 27251382
10. Inder TE, Volpe JJ. Mechanisms of perinatal brain injury. *Seminars in neonatology*: SN. 2000; 5(1):3–16. <https://doi.org/10.1053/siny.1999.0112> PMID: 10802746
11. McLean C, Ferriero D. Mechanisms of hypoxic-ischemic injury in the term infant. *Seminars in perinatology*. 2004; 28(6):425–32. PMID: 15693399
12. Mokni M, Hamlaoui S, Karkouch I, Amri M, Marzouki L, Limam F, et al. Resveratrol Provides Cardio-protection after Ischemia/reperfusion Injury via Modulation of Antioxidant Enzyme Activities. *Iranian Journal of Pharmaceutical Research: IJPR*. 2013; 12(4):867–75. PMID: 24523766
13. Youdim KA, Shukitt-Hale B, Joseph JA. Flavonoids and the brain: interactions at the blood-brain barrier and their physiological effects on the central nervous system. *Free radical biology & medicine*. 2004; 37(11):1683–93.
14. Aquilano K, Baldelli S, Rotilio G, Ciriolo MR. Role of nitric oxide synthases in Parkinson's disease: a review on the antioxidant and anti-inflammatory activity of polyphenols. *Neurochemical research*. 2008; 33(12):2416–26. <https://doi.org/10.1007/s11064-008-9697-6> PMID: 18415676
15. Bastianetto S, Krantic S, Quirion R. Polyphenols as potential inhibitors of amyloid aggregation and toxicity: possible significance to Alzheimer's disease. *Mini reviews in medicinal chemistry*. 2008; 8(5):429–35. PMID: 18473932
16. Esmailzadeh A, Tahbaz F, Gaieni I, Alavi-Majd H, Azadbakht L. Cholesterol-lowering effect of concentrated pomegranate juice consumption in type II diabetic patients with hyperlipidemia. *International journal for vitamin and nutrition research Internationale Zeitschrift für Vitamin- und Ernährungsforschung Journal international de vitaminologie et de nutrition*. 2006; 76(3):147–51. <https://doi.org/10.1024/0300-9831.76.3.147> PMID: 17048194
17. Hong MY, Seeram NP, Heber D. Pomegranate polyphenols down-regulate expression of androgen-synthesizing genes in human prostate cancer cells overexpressing the androgen receptor. *The Journal of nutritional biochemistry*. 2008; 19(12):848–55. <https://doi.org/10.1016/j.jnutbio.2007.11.006> PMID: 18479901
18. Shema-Didi L, Sela S, Ore L, Shapiro G, Geron R, Moshe G, et al. One year of pomegranate juice intake decreases oxidative stress, inflammation, and incidence of infections in hemodialysis patients: A randomized placebo-controlled trial. *Free Radical Biology and Medicine*. 2012; 53(2):297–304. <https://doi.org/10.1016/j.freeradbiomed.2012.05.013> PMID: 22609423
19. Heber D, Seeram NP, Wyatt H, Henning SM, Zhang Y, Ogden LG, et al. Safety and antioxidant activity of a pomegranate ellagitannin-enriched polyphenol dietary supplement in overweight individuals with increased waist size. *Journal of agricultural and food chemistry*. 2007; 55(24):10050–4. <https://doi.org/10.1021/jf071689v> PMID: 17966977
20. Seeram NP, Aviram M, Zhang Y, Henning SM, Feng L, Dreher M, et al. Comparison of antioxidant potency of commonly consumed polyphenol-rich beverages in the United States. *Journal of agricultural and food chemistry*. 2008; 56(4):1415–22. <https://doi.org/10.1021/jf0730305s> PMID: 18220345
21. Loren DJ, Seeram NP, Schulman RN, Holtzman DM. Maternal dietary supplementation with pomegranate juice is neuroprotective in an animal model of neonatal hypoxic-ischemic brain injury. *Pediatric research*. 2005; 57(6):858–64. <https://doi.org/10.1203/01.PDR.0000157722.07810.15> PMID: 15774834

22. West T, Atzeva M, Holtzman DM. Pomegranate polyphenols and resveratrol protect the neonatal brain against hypoxic-ischemic injury. *Developmental neuroscience*. 2007; 29(4–5):363–72. <https://doi.org/10.1159/000105477> PMID: 17762204
23. Chen B, Longtine MS, Nelson DM. Punicalagin, a polyphenol in pomegranate juice, downregulates p53 and attenuates hypoxia-induced apoptosis in cultured human placental syncytiotrophoblasts. *American journal of physiology Endocrinology and metabolism*. 2013; 305(10):E1274–80. <https://doi.org/10.1152/ajpendo.00218.2013> PMID: 24085032
24. Chen B, Tuuli MG, Longtine MS, Shin JS, Lawrence R, Inder T, et al. Pomegranate juice and punicalagin attenuate oxidative stress and apoptosis in human placenta and in human placental trophoblasts. *American journal of physiology Endocrinology and metabolism*. 2012; 302(9):E1142–52. <https://doi.org/10.1152/ajpendo.00003.2012> PMID: 22374759
25. Kingdom J, Smith G. Diagnosis and management of IUGR. In: Kingdom J, Baker P, editors. *Intrauterine Growth Restriction Aetiology and Management*. London: Springer; 2000. p. 257–73.
26. Resnik R. Intrauterine growth restriction. *Obstetrics and gynecology*. 2002; 99(3):490–6. PMID: 11864679
27. Miller SL, Huppi PS, Mallard C. The consequences of fetal growth restriction on brain structure and neurodevelopmental outcome. *The Journal of Physiology*. 2016; 594(4):807–23. <https://doi.org/10.1113/JP271402> PMID: 26607046
28. Lodygensky GA, Seghier ML, Warfield SK, Tolsa CB, Sizonenko S, Lazeyras F, et al. Intrauterine growth restriction affects the preterm infant's hippocampus. *Pediatric research*. 2008; 63(4):438–43. <https://doi.org/10.1203/PDR.0b013e318165c005> PMID: 18356754
29. Tolsa CB, Zimine S, Warfield SK, Freschi M, Sancho Rossignol A, Lazeyras F, et al. Early alteration of structural and functional brain development in premature infants born with intrauterine growth restriction. *Pediatric research*. 2004; 56(1):132–8. <https://doi.org/10.1203/01.PDR.0000128983.54614.7E> PMID: 15128927
30. American College of Obstetricians and Gynecologists. ACOG Practice bulletin no. 134: fetal growth restriction. *Obstetrics and gynecology*. 2013; 121(5):1122–33. <https://doi.org/10.1097/01.AOG.0000429658.85846.f9> PMID: 23635765
31. Ben Nasr C, Ayed N, Metche M. Quantitative determination of the polyphenolic content of pomegranate peel. *Zeitschrift für Lebensmittel-Untersuchung und -Forschung*. 1996; 203(4):374–8. PMID: 9123975
32. Singleton VL, Rossi JA. Colorimetry of Total Phenolics with Phosphomolybdic-Phosphotungstic Acid Reagents. 1965; 16(3):144–58.
33. Mathur AM, Neil JJ, McKinstry RC, Inder TE. Transport, monitoring, and successful brain MR imaging in unsedated neonates. *Pediatr Radiol*. 2008; 38(3):260–4. <https://doi.org/10.1007/s00247-007-0705-9> PMID: 18175110
34. Kidokoro H, Neil JJ, Inder TE. New MR imaging assessment tool to define brain abnormalities in very preterm infants at term. *AJNR American journal of neuroradiology*. 2013; 34(11):2208–14. <https://doi.org/10.3174/ajnr.A3521> PMID: 23620070
35. Nguyen The Tich S, Anderson PJ, Shimony JS, Hunt RW, Doyle LW, Inder TE. A novel quantitative simple brain metric using MR imaging for preterm infants. *AJNR American journal of neuroradiology*. 2009; 30(1):125–31. <https://doi.org/10.3174/ajnr.A1309> PMID: 18832662
36. Beare R, Chen J, Kelly C, Alexopoulos D, Smyser C, Rogers C, et al. Neonatal Brain Tissue Classification with Morphological Adaptation and Unified Segmentation. *Frontiers in Neuroinformatics*. 2016;10. <https://doi.org/10.3389/fninf.2016.00010>
37. Rogers CE, Smyser T, Smyser CD, Shimony J, Inder TE, Neil JJ. Regional white matter development in very preterm infants: perinatal predictors and early developmental outcomes. *Pediatric research*. 2016; 79(1–1):87–95. <https://doi.org/10.1038/pr.2015.172> PMID: 26372513
38. Smith SM, Jenkinson M, Woolrich MW, Beckmann CF, Behrens TE, Johansen-Berg H, et al. Advances in functional and structural MR image analysis and implementation as FSL. *NeuroImage*. 2004; 23 Suppl 1:S208–19.
39. Smyser CD, Inder TE, Shimony JS, Hill JE, Degnan AJ, Snyder AZ, et al. Longitudinal Analysis of Neural Network Development in Preterm Infants. *Cerebral Cortex (New York, NY)*. 2010; 20(12):2852–62.
40. Herzmann C, Snyder A, Kenley J, Rogers C, Shimony J, Smyser C. Cerebellar Functional Connectivity in Term- and Very Preterm-Born Infants. *Cerebral Cortex (New York, NY)*. 2018;<https://doi.org/10.1093/cercor/bhy023>.
41. Power JD, Barnes KA, Snyder AZ, Schlaggar BL, Petersen SE. Spurious but systematic correlations in functional connectivity MRI networks arise from subject motion. *NeuroImage*. 2012; 59(3):2142–54. <https://doi.org/10.1016/j.neuroimage.2011.10.018> PMID: 22019881

42. Smyser CD, Dosenbach NUF, Smyser TA, Snyder AZ, Rogers CE, Inder TE, et al. Prediction of brain maturity in infants using machine-learning algorithms. *NeuroImage*. 2016; 136:1–9. <https://doi.org/10.1016/j.neuroimage.2016.05.029> PMID: 27179605
43. Cohen AL, Fair DA, Dosenbach NUF, Miezin FM, Dierker D, Van Essen DC, et al. Defining Functional Areas in Individual Human Brains using Resting Functional Connectivity MRI. *NeuroImage*. 2008; 41(1):45–57. <https://doi.org/10.1016/j.neuroimage.2008.01.066> PMID: 18367410
44. Power JD, Cohen AL, Nelson SM, Wig GS, Barnes KA, Church JA, et al. Functional network organization of the human brain. *Neuron*. 2011; 72(4):665–78. <https://doi.org/10.1016/j.neuron.2011.09.006> PMID: 22099467
45. Smyser CD, Snyder AZ, Shimony JS, Mitra A, Inder TE, Neil JJ. Resting-State Network Complexity and Magnitude Are Reduced in Prematurely Born Infants. *Cerebral cortex (New York, NY: 1991)*. 2016; 26(1):322–33.
46. Jenkins G, Watts D. *Spectral Analysis and Its Applications*. San Francisco, CA: Holden-Day; 1968.
47. Smyser CD, Snyder AZ, Shimony JS, Blazey TM, Inder TE, Neil JJ. Effects of white matter injury on resting state fMRI measures in prematurely born infants. *PloS one*. 2013; 8(7):e68098. <https://doi.org/10.1371/journal.pone.0068098> PMID: 23874510
48. Brier M, Thomas JB, Snyder AZ, Benzinger TL, Zhang D, Raichle ME, et al. Loss of Intra- and Inter-Network Resting State Functional Connections with Alzheimer's Disease Progression. *The Journal of neuroscience: the official journal of the Society for Neuroscience*. 2012; 32(26):8890–9.
49. Papile LA, Burstein J, Burstein R, Koffler H. Incidence and evolution of subependymal and intraventricular hemorrhage: a study of infants with birth weights less than 1,500 gm. *The Journal of pediatrics*. 1978; 92(4):529–34. [https://doi.org/10.1016/s0022-3476\(78\)80282-0](https://doi.org/10.1016/s0022-3476(78)80282-0) PMID: 305471
50. Inder TE, Warfield SK, Wang H, Huppi PS, Volpe JJ. Abnormal cerebral structure is present at term in premature infants. *Pediatrics*. 2005; 115(2):286–94. <https://doi.org/10.1542/peds.2004-0326> PMID: 15687434
51. Bender R, Lange S. Adjusting for multiple testing—when and how? *Journal of clinical epidemiology*. 2001; 54(4):343–9. PMID: 11297884
52. Rothman KJ. No adjustments are needed for multiple comparisons. *Epidemiology*. 1990; 1(1):43–6. PMID: 2081237
53. Olsen IE, Groveman SA, Lawson ML, Clark RH, Zemel BS. New intrauterine growth curves based on United States data. *Pediatrics*. 2010; 125(2):e214–24. <https://doi.org/10.1542/peds.2009-0913> PMID: 20100760
54. Ginsberg Y, Khatib N, Saadi N, Ross MG, Weiner Z, Beloosesky R. Maternal pomegranate juice attenuates maternal inflammation-induced fetal brain injury by inhibition of apoptosis, neuronal nitric oxide synthase, and NF-kappaB in a rat model. *American journal of obstetrics and gynecology*. 2018; 219(1):113.e1–e9.
55. Chen B, Longtine MS, Riley JK, Nelson DM. Antenatal pomegranate juice rescues hypoxia-induced fetal growth restriction in pregnant mice while reducing placental cell stress and apoptosis. *Placenta*. 2018; 66:1–7. <https://doi.org/10.1016/j.placenta.2018.04.009> PMID: 29884297
56. Gluckman PD, Wyatt JS, Azzopardi D, Ballard R, Edwards AD, Ferriero DM, et al. Selective head cooling with mild systemic hypothermia after neonatal encephalopathy: multicentre randomised trial. *Lancet (London, England)*. 2005; 365(9460):663–70.
57. Spittle AJ, Doyle LW, Anderson PJ, Inder TE, Lee KJ, Boyd RN, et al. Reduced cerebellar diameter in very preterm infants with abnormal general movements. *Early Hum Dev*. 2010; 86(1):1–5. <https://doi.org/10.1016/j.earlhumdev.2009.11.002> PMID: 20004536
58. Lawrence RK, Inder TE. Anatomic Changes and Imaging in Assessing Brain Injury in the Term Infant. *Clinics in Perinatology*. 2008; 35(4):679–vi. <https://doi.org/10.1016/j.clp.2008.07.013> PMID: 19026334
59. de Vries LS, Groenendaal F. Patterns of neonatal hypoxic–ischaemic brain injury. *Neuroradiology*. 2010; 52(6):555–66. <https://doi.org/10.1007/s00234-010-0674-9> PMID: 20390260
60. Panickar KS, Anderson RA. Effect of polyphenols on oxidative stress and mitochondrial dysfunction in neuronal death and brain edema in cerebral ischemia. *Int J Mol Sci*. 2011; 12(11):8181–207. <https://doi.org/10.3390/ijms12118181> PMID: 22174658
61. Lee H, Bae JH, Lee SR. Protective effect of green tea polyphenol EGCG against neuronal damage and brain edema after unilateral cerebral ischemia in gerbils. *Journal of neuroscience research*. 2004; 77(6):892–900. <https://doi.org/10.1002/jnr.20193> PMID: 15334607
62. Lee S, Suh S, Kim S. Protective effects of the green tea polyphenol (-)-epigallocatechin gallate against hippocampal neuronal damage after transient global ischemia in gerbils. *Neuroscience letters*. 2000; 287(3):191–4. [https://doi.org/10.1016/s0304-3940\(00\)01159-9](https://doi.org/10.1016/s0304-3940(00)01159-9) PMID: 10863027

63. Park JW, Jang YH, Kim JM, Lee H, Park WK, Lim MB, et al. Green tea polyphenol (-)-epigallocatechin gallate reduces neuronal cell damage and up-regulation of MMP-9 activity in hippocampal CA1 and CA2 areas following transient global cerebral ischemia. *Journal of neuroscience research*. 2009; 87(2):567–75. <https://doi.org/10.1002/jnr.21847> PMID: 18752302
64. Ritz MF, Ratajczak P, Curin Y, Cam E, Mendelowitsch A, Pinet F, et al. Chronic treatment with red wine polyphenol compounds mediates neuroprotection in a rat model of ischemic cerebral stroke. *The Journal of nutrition*. 2008; 138(3):519–25. <https://doi.org/10.1093/jn/138.3.519> PMID: 18287360
65. Shukla PK, Khanna VK, Ali MM, Khan MY, Srimal RC. Anti-ischemic effect of curcumin in rat brain. *Neurochemical research*. 2008; 33(6):1036–43. <https://doi.org/10.1007/s11064-007-9547-y> PMID: 18204970
66. Simao F, Matte A, Matte C, Soares FM, Wyse AT, Netto CA, et al. Resveratrol prevents oxidative stress and inhibition of Na(+)/K(+)-ATPase activity induced by transient global cerebral ischemia in rats. *The Journal of nutritional biochemistry*. 2011; 22(10):921–8. <https://doi.org/10.1016/j.jnutbio.2010.07.013> PMID: 21208792
67. Della-Morte D, Dave KR, DeFazio RA, Bao YC, Raval AP, Perez-Pinzon MA. Resveratrol pretreatment protects rat brain from cerebral ischemic damage via a sirtuin 1-uncoupling protein 2 pathway. *Neuroscience*. 2009; 159(3):993–1002. <https://doi.org/10.1016/j.neuroscience.2009.01.017> PMID: 19356683
68. Zhao HF, Li N, Wang Q, Cheng XJ, Li XM, Liu TT. Resveratrol decreases the insoluble A β 1–42 level in hippocampus and protects the integrity of the blood–brain barrier in AD rats. *Neuroscience*. 2015; 310:641–9. <https://doi.org/10.1016/j.neuroscience.2015.10.006> PMID: 26454022
69. Salberg S, Yamakawa G, Christensen J, Kolb B, Mychasiuk R. Assessment of a nutritional supplement containing resveratrol, prebiotic fiber, and omega-3 fatty acids for the prevention and treatment of mild traumatic brain injury in rats. *Neuroscience*. 2017; 365:146–57. <https://doi.org/10.1016/j.neuroscience.2017.09.053> PMID: 28988852
70. Chahboune H, Ment LR, Stewart WB, Rothman DL, Vaccarino FM, Hyder F, et al. Hypoxic injury during neonatal development in murine brain: correlation between in vivo DTI findings and behavioral assessment. *Cerebral cortex (New York, NY: 1991)*. 2009; 19(12):2891–901. <https://doi.org/10.1093/cercor/bhp068> PMID: 19380380
71. Jones DK, Knösche TR, Turner R. White matter integrity, fiber count, and other fallacies: The do's and don'ts of diffusion MRI. *NeuroImage*. 2013; 73:239–54. <https://doi.org/10.1016/j.neuroimage.2012.06.081> PMID: 22846632
72. Wozniak JR, Lim KO. Advances in white matter imaging: a review of in vivo magnetic resonance methodologies and their applicability to the study of development and aging. *Neurosci Biobehav Rev*. 2006; 30(6):762–74. <https://doi.org/10.1016/j.neubiorev.2006.06.003> PMID: 16890990
73. Li K, Sun Z, Han Y, Gao L, Yuan L, Zeng D. Fractional anisotropy alterations in individuals born preterm: a diffusion tensor imaging meta-analysis. *Developmental Medicine & Child Neurology*. 2015; 57(4):328–38.
74. Taoka T, Kin T, Nakagawa H, Hirano M, Sakamoto M, Wada T, et al. Diffusivity and diffusion anisotropy of cerebellar peduncles in cases of spinocerebellar degenerative disease. *NeuroImage*. 2007; 37(2):387–93. <https://doi.org/10.1016/j.neuroimage.2007.05.028> PMID: 17583535
75. Mukherjee P, Miller J. Diffusion tensor MR imaging of gray and white matter development during normal human brain maturation. *AJNR American journal of neuroradiology*. 2002; 23(9):1445–56. PMID: 12372731
76. Smyser TA, Smyser CD, Rogers CE, Gillespie SK, Inder TE, Neil JJ. Cortical Gray and Adjacent White Matter Demonstrate Synchronous Maturation in Very Preterm Infants. *Cereb Cortex*. 2016; 26(8):3370–8. <https://doi.org/10.1093/cercor/bhv164> PMID: 26209848
77. Cascio CJ, Gerig G, Piven J. Diffusion Tensor Imaging: Application to the Study of the Developing Brain. *Journal of the American Academy of Child & Adolescent Psychiatry*. 2007; 46(2):213–23.
78. Gao W, Lin W, Chen Y, Gerig G, Smith JK, Jewells V, et al. Temporal and spatial development of axonal maturation and myelination of white matter in the developing brain. *AJNR American journal of neuroradiology*. 2009; 30(2):290–6. <https://doi.org/10.3174/ajnr.A1363> PMID: 19001533
79. Dulcich MS, Hartman RE. Pomegranate supplementation improves affective and motor behavior in mice after radiation exposure. *Evidence-based complementary and alternative medicine: eCAM*. 2013; 2013:940830.
80. Subash S, Braidy N, Essa MM, Zayana AB, Ragini V, Al-Adawi S, et al. Long-term (15 mo) dietary supplementation with pomegranates from Oman attenuates cognitive and behavioral deficits in a transgenic mice model of Alzheimer's disease. *Nutrition (Burbank, Los Angeles County, Calif)*. 2015; 31(1):223–9.

81. Braidy N, Essa MM, Poljak A, Selvaraju S, Al-Adawi S, Manivasagam T, et al. Consumption of pomegranates improves synaptic function in a transgenic mice model of Alzheimer's disease. *Oncotarget*. 2016; 7(40):64589–604. <https://doi.org/10.18632/oncotarget.10905> PMID: 27486879
82. Fox MD, Raichle ME. Spontaneous fluctuations in brain activity observed with functional magnetic resonance imaging. *Nature reviews Neuroscience*. 2007; 8(9):700–11. <https://doi.org/10.1038/nrn2201> PMID: 17704812
83. Meyer A. A note on the postnatal development of the human cerebral cortex. *Cerebral palsy bulletin*. 1961; 3:263–8. PMID: 13769948
84. Conel J. The postnatal development of the human cerebral cortex. Cambridge (MA): Harvard University Press; 1939.
85. Benjamini Y, Hochberg Y. Controlling the False Discovery Rate: A Practical and Powerful Approach to Multiple Testing. *Journal of the Royal Statistical Society Series B (Methodological)*. 1995; 57(1):289–300.
86. Ruzafa N, Rey-Santano C, Mielgo V, Pereiro X, Vecino E. Effect of hypoxia on the retina and superior colliculus of neonatal pigs. *PloS one*. 2017; 12(4):e0175301. <https://doi.org/10.1371/journal.pone.0175301> PMID: 28407001
87. Kaur C, Rathnasamy G, Ling EA. Roles of activated microglia in hypoxia induced neuroinflammation in the developing brain and the retina. *Journal of neuroimmune pharmacology: the official journal of the Society on NeuroImmune Pharmacology*. 2013; 8(1):66–78.
88. Rothman SM, Olney JW. Glutamate and the pathophysiology of hypoxic—ischemic brain damage. *Annals of neurology*. 1986; 19(2):105–11. <https://doi.org/10.1002/ana.410190202> PMID: 2421636
89. Murphy TH, Miyamoto M, Sastre A, Schnaar RL, Coyle JT. Glutamate toxicity in a neuronal cell line involves inhibition of cystine transport leading to oxidative stress. *Neuron*. 1989; 2(6):1547–58. PMID: 2576375
90. Hanneken A, Lin FF, Johnson J, Maher P. Flavonoids protect human retinal pigment epithelial cells from oxidative-stress-induced death. *Investigative ophthalmology & visual science*. 2006; 47(7):3164–77.
91. Maher P, Hanneken A. Flavonoids protect retinal ganglion cells from oxidative stress-induced death. *Investigative ophthalmology & visual science*. 2005; 46(12):4796–803.
92. Maher P, Hanneken A. The molecular basis of oxidative stress-induced cell death in an immortalized retinal ganglion cell line. *Investigative ophthalmology & visual science*. 2005; 46(2):749–57.
93. Nakayama M, Aihara M, Chen Y-N, Araie M, Tomita-Yokotani K, Iwashina T. Neuroprotective effects of flavonoids on hypoxia-, glutamate-, and oxidative stress-induced retinal ganglion cell death. *Molecular Vision*. 2011; 17:1784–93. PMID: 21753864
94. Andrews-Hanna JR, Snyder AZ, Vincent JL, Lustig C, Head D, Raichle ME, et al. Disruption of large-scale brain systems in advanced aging. *Neuron*. 2007; 56(5):924–35. <https://doi.org/10.1016/j.neuron.2007.10.038> PMID: 18054866
95. Fjell AM, Sneve MH, Storsve AB, Grydeland H, Yendiki A, Walhovd KB. Brain Events Underlying Episodic Memory Changes in Aging: A Longitudinal Investigation of Structural and Functional Connectivity. *Cerebral cortex (New York, NY)*. 2016; 26(3):1272–86.
96. Hirsiger S, Koppelmans V, Merillat S, Liem F, Erdeniz B, Seidler RD, et al. Structural and functional connectivity in healthy aging: Associations for cognition and motor behavior. *Human brain mapping*. 2016; 37(3):855–67. <https://doi.org/10.1002/hbm.23067> PMID: 26663386
97. Tsang A, Lebel CA, Bray SL, Goodyear BG, Hafeez M, Sotero RC, et al. White Matter Structural Connectivity Is Not Correlated to Cortical Resting-State Functional Connectivity over the Healthy Adult Lifespan. *Frontiers in Aging Neuroscience*. 2017; 9:144. <https://doi.org/10.3389/fnagi.2017.00144> PMID: 28572765
98. Honey CJ, Sporns O, Cammoun L, Gigandet X, Thiran JP, Meuli R, et al. Predicting human resting-state functional connectivity from structural connectivity. *Proceedings of the National Academy of Sciences*. 2009; 106(6):2035–40.
99. Espín JC, Larrosa M, García-Conesa MT, Tomás-Barberán F. Biological Significance of Urolithins, the Gut Microbial Ellagic Acid-Derived Metabolites: The Evidence So Far. *Evidence-based complementary and alternative medicine: eCAM*. 2013; 2013:270418.
100. Seeram NP, Henning SM, Zhang Y, Suchard M, Li Z, Heber D. Pomegranate juice ellagitannin metabolites are present in human plasma and some persist in urine for up to 48 hours. *The Journal of nutrition*. 2006; 136(10):2481–5. <https://doi.org/10.1093/jn/136.10.2481> PMID: 16988113
101. Cerda B, Espin JC, Parra S, Martinez P, Tomas-Barberan FA. The potent in vitro antioxidant ellagitannins from pomegranate juice are metabolised into bioavailable but poor antioxidant hydroxy-6H-

- dibenzopyran-6-one derivatives by the colonic microflora of healthy humans. *European journal of nutrition*. 2004; 43(4):205–20. <https://doi.org/10.1007/s00394-004-0461-7> PMID: 15309440
102. Mertens-Talcott SU, Jilma-Stohlawetz P, Rios J, Hingorani L, Derendorf H. Absorption, metabolism, and antioxidant effects of pomegranate (*Punica granatum* L.) polyphenols after ingestion of a standardized extract in healthy human volunteers. *Journal of agricultural and food chemistry*. 2006; 54(23):8956–61. <https://doi.org/10.1021/jf061674h> PMID: 17090147
 103. Tomas-Barberan FA, Selma MV, Espin JC. Interactions of gut microbiota with dietary polyphenols and consequences to human health. *Current opinion in clinical nutrition and metabolic care*. 2016; 19(6):471–6. <https://doi.org/10.1097/MCO.0000000000000314> PMID: 27490306
 104. Hammerstone JF, Lazarus SA, Schmitz HH. Procyanidin content and variation in some commonly consumed foods. *The Journal of nutrition*. 2000; 130(8S Suppl):2086s–92s. <https://doi.org/10.1093/jn/130.8.2086S> PMID: 10917927
 105. Lacroix S, Klicic Badoux J, Scott-Boyer MP, Parolo S, Matone A, Priami C, et al. A computationally driven analysis of the polyphenol-protein interactome. *Scientific reports*. 2018; 8(1):2232. <https://doi.org/10.1038/s41598-018-20625-5> PMID: 29396566